Distinct Hydrological Signatures in Observed Historical Temperature Fields

RANDAL D. KOSTER, MAX J. SUAREZ, AND SIEGFRIED D. SCHUBERT

Global Modeling and Assimilation Office, NASA Goddard Space Flight Center, Greenbelt, Maryland

(Manuscript received 22 July 2005, in final form 28 December 2005)

ABSTRACT

In an atmospheric general circulation model (AGCM), the physical bounds on soil moisture content and the nonlinear relationship between soil moisture and evaporation lead to distinct geographical patterns in key surface energy and water balance variables. In particular, simple hydrological considerations suggest—and extensive AGCM simulations confirm—that the variance and skew of seasonally averaged [June–August (JJA)] air temperature on the planet should be maximized in specific, and different, regions: a variance maximum should appear on the dry side of the soil moisture variance maximum, and a positive skew maximum should appear on the wet side of the temperature variance maximum. These ideas are tested with multidecade observational temperature data from the Global Historical Climatology Network (GHCN). In the United States, where sufficient data exist, the predicted patterns in the seasonal temperature moments show up where expected. These results suggest that hydrological considerations do indeed control the patterns of seasonal temperature variance and skew in nature.

1. Introduction

The characterization of the variability of earth's climate has always been limited by insufficient data. Most global datasets are limited to the satellite era (i.e., covering about 25 yr or less), and only a handful of high-resolution, spatially complete regional datasets span 50 yr or more [e.g., the U.S. rainfall dataset of Higgins et al. (2000)]. A few sources provide spatially limited data covering the last century [e.g., the Global Historical Climatology Network (GHCN) dataset (Peterson and Vose 1997)]. While 100 yr of data may seem substantial, it is insufficient for determining with confidence the higher moments of interannual climate variability. Going back much further than 100 yr requires the proper interpretation of climate proxies such as water isotope concentrations and tree ring thicknesses. These proxies are spatially limited, and their correlations with climate variables are far from perfect.

Numerical simulations of earth's climate with atmospheric general circulation models (AGCMs), on the other hand, can span thousands of years, providing extensive and comprehensive datasets. AGCMs, of course, have well-known flaws; even the best models produce large biases in simulated climate variables. Nevertheless, if care is taken in the analysis of their behavior, the models can reveal important physical mechanisms that control climate and its temporal variability.

One element of climate variability addressed by many recent AGCM studies is the impact of the land surface on the atmosphere, particularly the impact of soil moisture variations on precipitation generation and air temperature. Demonstrating that such land–atmosphere feedback exists in an AGCM is straightforward. While the strength of the simulated land–atmosphere connection varies significantly between AGCMs (Koster et al. 2006; Guo et al. 2006), models tend to agree that atmospheric processes do respond to anomalies in surface moisture conditions (Delworth and Manabe 1989; Beljaars et al. 1996; Fennessy and Shukla 1999; Douville and Chauvin 2000; Dirmeyer 2000; and many other studies). On the other hand, demonstrating unequivocally that land–atmosphere feedback occurs in nature is much more difficult. The observational record is both spatially and temporally inadequate for this purpose. Decadal soil moisture observations are essentially limited to point measurements in Asia and Illinois, and large-scale measurements of evaporation and sensible heat fluxes—the processes that link soil moisture to the atmosphere—do not exist across decades. Even if the

Corresponding author address: Randal Koster, Global Modeling and Assimilation Office, Code 610.1, NASA Goddard Space Flight Center, Greenbelt, MD 20771.
E-mail: randal.d.koster@nasa.gov

measurements were complete in space and time, diagnosing directions of causality can be very difficult given the complex nature of the land–atmosphere system. For example, any observed concurrence of high rainfall rates and high soil moisture values would probably reflect rainfall's impact on soil moisture rather than the other way around, and lagged analyses of the variables are clouded by the potential for externally induced persistence in the rainfall.

These problems can be circumvented to some extent by using an AGCM as a tool in the search for observational evidence of land–atmosphere feedback. The basic approach is as follows. First, a feature in the observations suspected of being a signature of the feedback is identified. Then, the presence of the feature is sought in the AGCM output. If it does appear in the model, carefully designed sensitivity studies are used to determine whether or not land–atmosphere feedback is indeed responsible for it. Demonstration that feedback causes the feature in the AGCM supports (though does not prove) the supposition that feedback is responsible for the feature in the real world as well. Studies following some form of this approach include those of Huang and Van den Dool (1993), who examined one-month-lagged correlations between precipitation and temperature; Koster et al. (2003), who examined precipitation autocorrelation patterns in the continental United States; Koster and Suarez (2004), who examined midlatitude precipitation totals conditioned on totals in previous months; and Koster et al. (2004), who demonstrated that the realistic initialization of soil moisture in a forecast model leads to improved subseasonal precipitation and air temperature forecasts.

The present paper adds to this series, finding signals of land–atmosphere feedback in a different observational dataset, one previously untapped for this purpose. The data examined here are the multidecade air temperature records archived by the Global Historical Climatology Network (Peterson and Vose 1997). Relationships are identified between the statistical moments of seasonally averaged air temperature and soil moisture, relationships that can be expected in the observations only if feedback is important in the real world—only if the other factors controlling temperature do not overwhelm the feedback signal.

We emphasize that the relationships identified and sought for in the observational temperature record are subtle, going well beyond the trivial notion that wetter conditions imply cooler temperatures. In fact, these subtle relationships allow us to test for more than just the existence of feedback; they allow us to examine the behavior of real-world evaporation. Conventional wisdom, based on theory and some local site measurements (Budyko 1974; Manabe 1969; Eagleson 1978), suggests that evaporation increases with soil moisture for drier soils only. Evaporation is insensitive to soil moisture for wetter soils, for which the evaporation rate is controlled instead by atmospheric demand. Such behavior is usually built directly into the evaporation formulations used by AGCMs. It has never, however, been tested with real-world data at the regional to continental scale, mostly due to the aforementioned paucity of large-scale evaporation and soil moisture measurements. Because the temperature signals we identify follow directly from the idea that evaporation has two regimes, one controlled by soil moisture and the other controlled by atmospheric demand, the large-scale observational temperature record provides a unique opportunity to demonstrate the relevance of these two regimes and thus the correctness of the models' imposed evaporation behavior.

Of course, the discovery of these signals—these unique feedback "signatures"—in the observational data cannot prove anything conclusively, since their appearance could be a coincidence or a statistical fluke. Nevertheless, the presence of the expected signals can provide one more crucial piece of evidence that land–atmosphere feedback occurs in nature and that typical AGCM evaporation formulations are realistic. As discussed above, such observational evidence is very difficult to come by objectively, so each available piece of evidence—especially if derived from a previously untapped dataset—is of significant value.

Following a brief description of the AGCM simulations examined (section 2), this paper shows how the statistical moments of evaporation, and thus temperature, are influenced by soil moisture boundaries and by the relationship of evaporation to soil moisture (section 3). In section 4, these signatures are sought in the available observational data.

2. Models used and data analyzed

We use for this analysis the AGCM component of the seasonal forecast system of the Global Modeling and Assimilation Office of the National Aeronautics and Space Administration (NASA). [In earlier studies, this AGCM was referred to as the NASA Seasonal-to-Interannual Prediction Project (NSIPP) AGCM.] The $2^\circ \times 2.5^\circ$ finite-difference model uses the relaxed Arakawa–Schubert scheme (Moorthi and Suarez 1992) for convection and the treatments of Chou and Suarez (1994, 1996) for shortwave and longwave radiation, with an Earth Radiation Budget Experiment (ERBE)- and International Satellite Cloud Climatology Project (ISSCP)-based calibration of the cloud parameterization scheme. A fourth-order advection scheme is used

for vorticity and all scalars in the modeled dynamics. All land surface calculations are performed with the Mosaic scheme of Koster and Suarez (1996), a soil–vegetation–atmosphere transfer (SVAT) scheme that uses tiling to account for subgrid vegetation distributions. The coupled land–atmosphere system captures well the broad features of the climate system and the global hydrological cycle (Bacmeister et al. 2000; Koster et al. 2000).

To ensure reasonable statistics, we examine soil moisture, evaporation, and air temperature data spanning over 600 yr of simulation—the data are extracted from nine parallel Atmospheric Model Intercomparison Project (AMIP)-style simulations covering the period 1930–2003. To filter out some higher-frequency effects—the fact, for example, that synoptic-scale weather can affect air temperature without regard to soil moisture—all quantities are averaged across boreal summer months [June–August (JJA)] before being analyzed. We thus focus on soil moisture's influence over slow (seasonal) air temperature variability, during a season for which evaporation, and thus feedback with the atmosphere, should be maximized.

3. Model results

To illustrate the feedback signatures that may appear in a temperature record, we show in this section how the hydrological formulations imposed in an AGCM imply relationships between the statistical moments of soil moisture, evaporation, and temperature. Some of these relationships are intuitive, while others are more subtle. All, however, are indeed shown to be present in the AGCM's output diagnostics.

a. Soil moisture moments

Unlike temperature, precipitation, wind speed, and most other climate variables, soil moisture content (w, expressed as a degree of saturation) has very sharp upper and lower bounds. By definition, it cannot dip below 0, the value for a perfectly dry soil, and it cannot exceed 1, the value for a fully saturated soil. Indeed, most models effectively impose more stringent bounds associated with wilting and runoff processes (Koster and Milly 1997).

The existence of these physical bounds has a direct impact on the statistical moments of w. The impact on the third moment, the skew, is perhaps easiest to see. Consider a region with a time-averaged soil moisture close to the lower bound. The soil moisture will be constrained by this bound during years of low precipitation, but it will be unconstrained during wetter-than-average years. This asymmetry results in a positive skew for the temporal distribution. Similarly, if the average soil moisture at a given grid cell is close to the upper bound, soil moisture during the wetter-than-average years will be constrained, whereas that during the dryer-than-average years will be unconstrained, resulting in a negative skew.

The second moment, the variance, of soil moisture content is also affected. The lower physical bound implies that soil moisture contents in dry regions have a limited ability to vary, at least in the dry direction. Soil moisture variance there should thus be suppressed. Variance similarly should be reduced in wet regions, since soil moisture contents there cannot vary much in the wet direction. Another way to see this is to consider soil moisture as an integrator of antecedent rainfall and the two soil moisture bounds as "absorbing states" for the integration. Consider first a hypothetical wet region, one with a high JJA precipitation variance. In this hypothetical region, the rainfall varies greatly from year to year—it may be 8 mm day^{-1} in some years and 20 mm day^{-1} in others—yet it remains high enough in all years to keep the soil moisture near the saturated value, resulting in a high mean soil moisture but a low interannual soil moisture variance. The corresponding example for the dry case involves a region with consistently low precipitation, leading to both a low mean and a low variance of soil moisture. Intuitively, variance should be maximized in regions of intermediate wetness.

These arguments, though overly simple, are fully supported by the AGCM diagnostics. The histograms in Fig. 1 show how the variance and skew of AGCM-generated seasonally averaged (JJA) soil moisture varies with the climatological mean seasonal soil moisture $\overline{w}$. The binned averages are computed from midlatitude land points (30°–60°N). [We focus on midlatitudes in this paper to avoid the large impacts of interannually varying sea surface temperatures (SSTs) on tropical precipitation and temperature fields—we seek here to isolate and identify land effects.] Soil moisture variance is maximized for intermediate soil moisture values and approaches zero toward the dry and wet ends of the operating soil moisture range. The skew of soil moisture is clearly positive on the dry end and negative on the wet end. The skew approaches zero at the extremes because it scales with variance to the 3/2 power.

We say that these arguments are overly simple because the soil moisture moments are also controlled in large part by the moments of precipitation, the dominant driver of soil moisture. Precipitation, which cannot be negative, typically has positive skew; this may explain why the positive soil moisture skew in dry areas is larger than the negative soil moisture skew in wet areas (bottom panel of Fig. 1). Furthermore, precipitation is

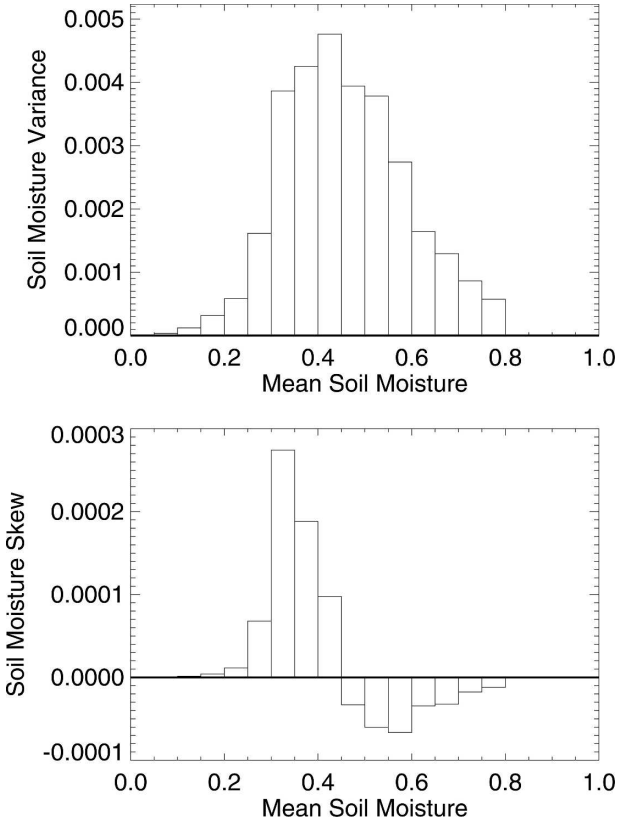

FIG. 1. (top) Average relationship between the variance of soil moisture and mean soil moisture, as determined from hundreds of years of AGCM simulations. To generate the histogram, midlatitude land points are binned according to their mean soil moisture (bin size = 0.05), and the average variance is computed for each set of binned points. (bottom) Same as top, but for the relationship between soil moisture skew and mean soil moisture. The soil moisture contents analyzed are JJA averages and are expressed in terms of degree of saturation.

known to be very responsive to variations in soil moisture in this AGCM, particularly in regions of intermediate soil moisture content (Koster et al. 2000, 2003). This means that the relationships seen in Fig. 1 reflect in part an amplification, through feedback, of the relationships originally established by the presence of the soil moisture bounds.

Regardless of their source, the soil moisture moment relationships in Fig. 1 do exist in the AGCM. As will be seen below, some simple hydrological considerations allow us to translate these relationships into corresponding relationships for the moments of air temperature in the AGCM.

b. The relationship between evaporation and soil moisture

Before looking at the evaporation and temperature moments, we must illustrate the underlying relationship

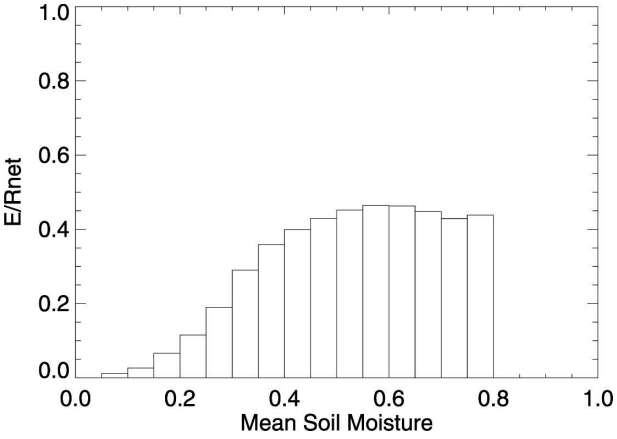

FIG. 2. Average relationship between the evaporative fraction and mean soil moisture, as determined from hundreds of years of AGCM simulations. To generate the histogram, midlatitude land points are binned according to their mean soil moisture, and the average value of E/R_{net} is computed for each set of binned points.

in the model between soil moisture and evaporation fraction (E/R_{net}, where E is total evaporation and R_{net} is the net radiation). The histogram in Fig. 2 shows this relationship for AGCM land cells in Northern Hemisphere midlatitudes. In the AGCM, evaporative fraction tends to increase with soil moisture up to a certain point ($w \approx 0.5$); above this point, the evaporative fraction is largely insensitive to soil moisture. Put simply, in the wetter regime, the soil can provide moisture to the atmosphere faster than the atmosphere can remove it. Note that the plateau at the wet end is not perfectly flat, presumably due to the mix of vegetation types considered and the relatively small number of points contributing to the highest bins. (Substantial scatter is seen prior to the binning.) Corresponding curves conditioned on vegetation type (Mahanama and Koster 2005) show much flatter plateaus, as expected.

As discussed in section 1, the characterization of two distinct regimes for evaporation—the drier, soil-moisture-controlled regime and the wetter, atmosphere-controlled regime—has a substantial heritage in the literature (e.g., Budyko 1974; Manabe 1969; Eagleson 1978). In other words, the presence of two separate regimes in Fig. 2 is neither a new result nor a unique model characteristic; the coexistence of the two regimes has long been assumed for the real world and is indeed effectively imposed in many models.

c. Hydrological signatures on evaporation moments

The dependence of evaporation variance on mean soil moisture can be deduced directly from the relationships in Figs. 1 and 2. Consider first the dry, soil-moisture-controlled evaporation regime. In this regime,

soil moisture variations lead to evaporation variations; a large soil moisture variance thus translates to a large evaporation variance. In contrast, in the wet (atmosphere controlled) regime, soil moisture variations do not lead to evaporation variations, and evaporation variance is necessarily quashed. Points near the transition moisture value ($\overline{w} \approx 0.5$) should also be reduced somewhat, since variations during wet years are not large. Based on these considerations, we might expect the relationship between evaporation variance and $\overline{w}$ to look like that between soil moisture variance and $\overline{w}$ (top panel of Fig. 1), but with much reduced variance for wetter conditions (i.e., the right part of the histogram pushed down toward zero).

The top two panels of Fig. 3 show that for the AGCM, this is indeed the case. The variance of evaporation is close to zero for $\overline{w}$ greater than about 0.5. Note that it need not be exactly zero, even for very wet conditions, since evaporation also varies with, for example, incident energy. (In fact, if we were to look at much finer time scales, such as daily values, radiation variations would induce much stronger evaporation variances, even for very wet soils. The shape of the distribution in the middle panel of Fig. 3 is appropriate for longer time scales only.) Because of the quashing of evaporation variance on the wet end, the maximum evaporation variance occurs at $\overline{w} \approx 0.33$, on the dry side of the maximum of the soil moisture variance.

The soil moisture–evaporation relationship also has a profound impact on the skew of evaporation. In wet areas ($\overline{w}$ close to 1), where evaporation does not vary with soil moisture, skew in soil moisture does not translate to skew in evaporation—the skew of evaporation is quashed, just as the variance is quashed. In dry areas ($\overline{w}$ close to 0), on the other hand, evaporation does vary with soil moisture, and soil moisture skew does lead to a corresponding skew in evaporation. Now consider intermediate soil moisture values (those near the transition point between soil-moisture-controlled and atmosphere-controlled regimes, at $\overline{w} \approx 0.5$), for which the shape of the histogram in Fig. 2 has a very interesting effect. Due to this shape, increases in evaporation during wetter-than-average years will be much smaller than decreases during drier-than-average years. This induces a strong negative skew in the evaporation.

The top two panels of Fig. 4 show the relationships between $\overline{w}$ and both soil moisture skew and evaporation skew. All three effects—the direct translation of skew for low $\overline{w}$, the imposition of negative evaporation skew (or, at the very least, a reduction of positive skew) for intermediate $\overline{w}$, and the quashing of evaporation skew for high $\overline{w}$—are captured by the AGCM. The overlain dashed lines show how the resulting extrema of evaporation skew are shifted from the corresponding extrema of the soil moisture skew.

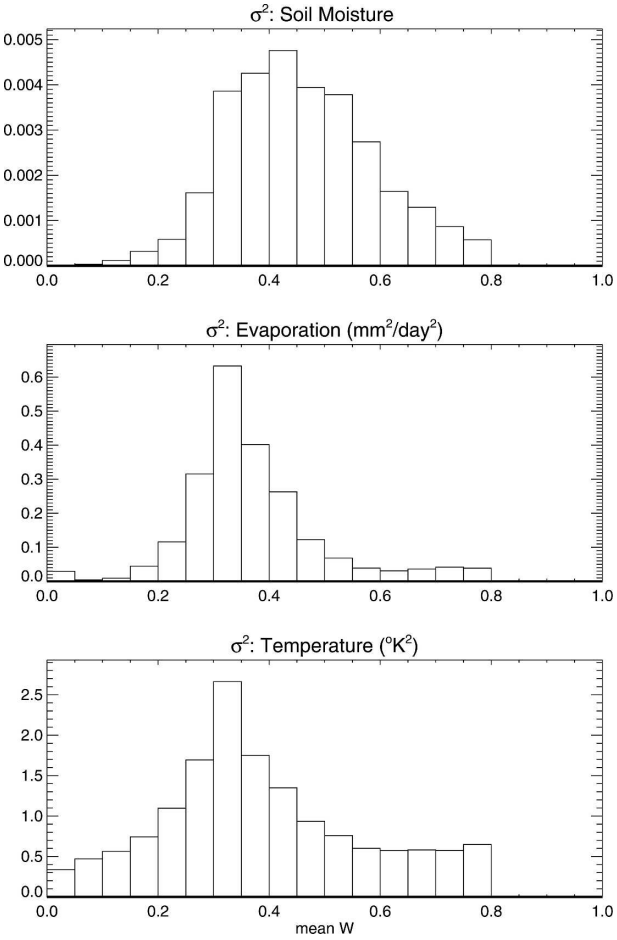

FIG. 3. (top) Average relationship between the variance of soil moisture and mean soil moisture, as determined from hundreds of years of AGCM simulations. To generate the histogram, midlatitude land points are binned according to their mean soil moisture (bin size = 0.05), and the average variance is computed for each set of binned points. (middle) Same as top, but for the relationship between evaporation variance and mean soil moisture. (bottom) Same as top, but for the relationship between temperature variance and mean soil moisture. The soil moisture contents analyzed are JJA averages and are expressed in terms of degree of saturation.

d. Hydrological signatures on temperature moments

The bottom panels of Figs. 3 and 4 show the relationships between $\overline{w}$ and the temperature moments. The overall shapes of the relationships, including the locations of the extrema, agree strongly with those for the evaporation moments. Visual inspection of Fig. 5 shows that evaporation and temperature moments are indeed strongly correlated across the globe. This is not a coincidence. Seasonally averaged (JJA) temperature

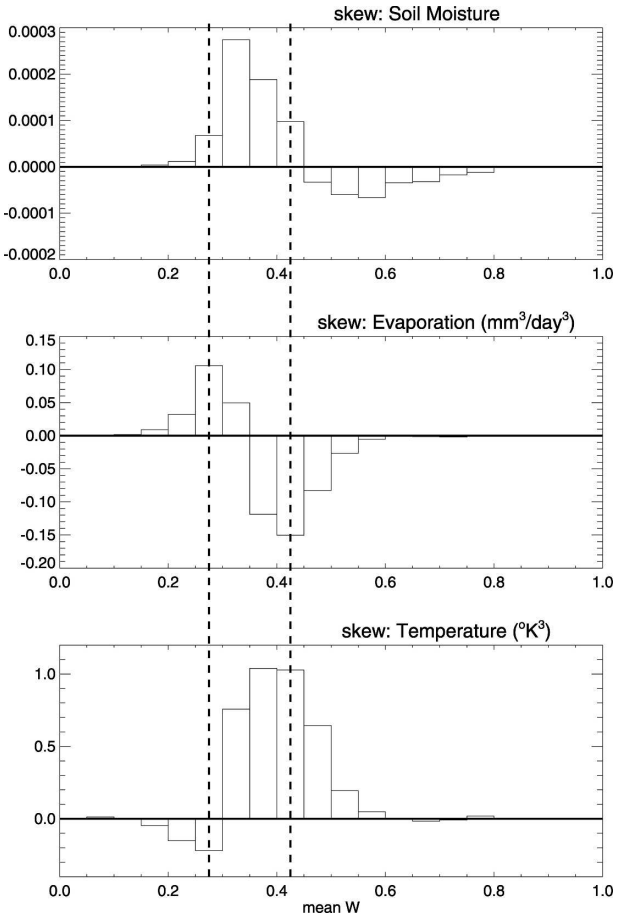

FIG. 4. Same as in Fig. 3, but for skew.

anomalies tend to be strongly (and negatively) correlated with seasonally averaged evaporation anomalies, particularly when the latter are large due to soil moisture variations. The correlation is due in large part to evaporative cooling—when more of the incident energy over the season is used to evaporate water, less is available to heat up the surface. Simply put, by determining the controls on the moments of seasonal evaporation, particularly for summer, we automatically determine critical controls on the moments of seasonal temperature.

To demonstrate more conclusively that the hydrological mechanisms outlined in sections 3a and 3b are responsible for the behavior of the temperature moments, we show in Fig. 6 a comparison of the moments from the AGCM with those from a supplemental run, one in which the land's impact on atmospheric variability is artificially disabled. In this supplemental run, we prescribe climatological, seasonally varying evaporation efficiencies (i.e., ratios between evaporation and potential evaporation) at the land surface rather than allow soil moisture, and thus evaporation, to increase following precipitation events. This "fixed β" approach is described in more detail by Koster et al. (2000). As in the original simulation, the SSTs in this 50-yr fixed-β simulation vary from year to year, giving ocean variability the opportunity to affect the continental temperature moments. By design, soil moisture data are not produced in the fixed-β run; the effective mean moistures, however, are the same as those for the control AGCM simulations.

Figure 6 shows that when the coupling of surface hydrological variables to the atmosphere is disabled, all hints of the temperature moment structure disappear. Thus, the air temperature moment structures in the AGCM are indeed fully induced by the coupling (and not, e.g., by SST variability), presumably through the mechanisms outlined above—mechanisms involving soil moisture bounds and the shape of the evaporation–soil moisture relationship.

To summarize, then, simple hydrological considerations suggest three distinct signatures of hydrological impacts on seasonal (JJA) temperature distributions, signatures that appear, as expected, in the AGCM data and can also be sought in the observational record. These are as follows.

(i) The temperature variance maximum should lie on the dry side of the soil moisture variance maximum, when both are plotted against mean soil moisture (Fig. 3).
(ii) The temperature skew should be large and positive on the wet side of the temperature variance maximum, when both are plotted against mean soil moisture (Fig. 7).
(iii) The temperature skew should be negative on the dry side of the temperature variance maximum, when both are plotted against mean soil moisture (Fig. 7).

Alternatively, for a continental region such as the United States with a distinct west-to-east gradient of soil moisture, maps of soil moisture and temperature moments should show the temperature variance maximum to the west of the soil moisture variance maximum, and they should show positive and negative temperature skew to the east and west, respectively, of the temperature variance maximum. In the next section, we will search for these structures in the observational temperature data, using observations-based soil moisture proxies.

4. Observations

The presence of the three identified feedback signatures in the AGCM data is not surprising, since the signatures follow directly from the model's imposed hy-

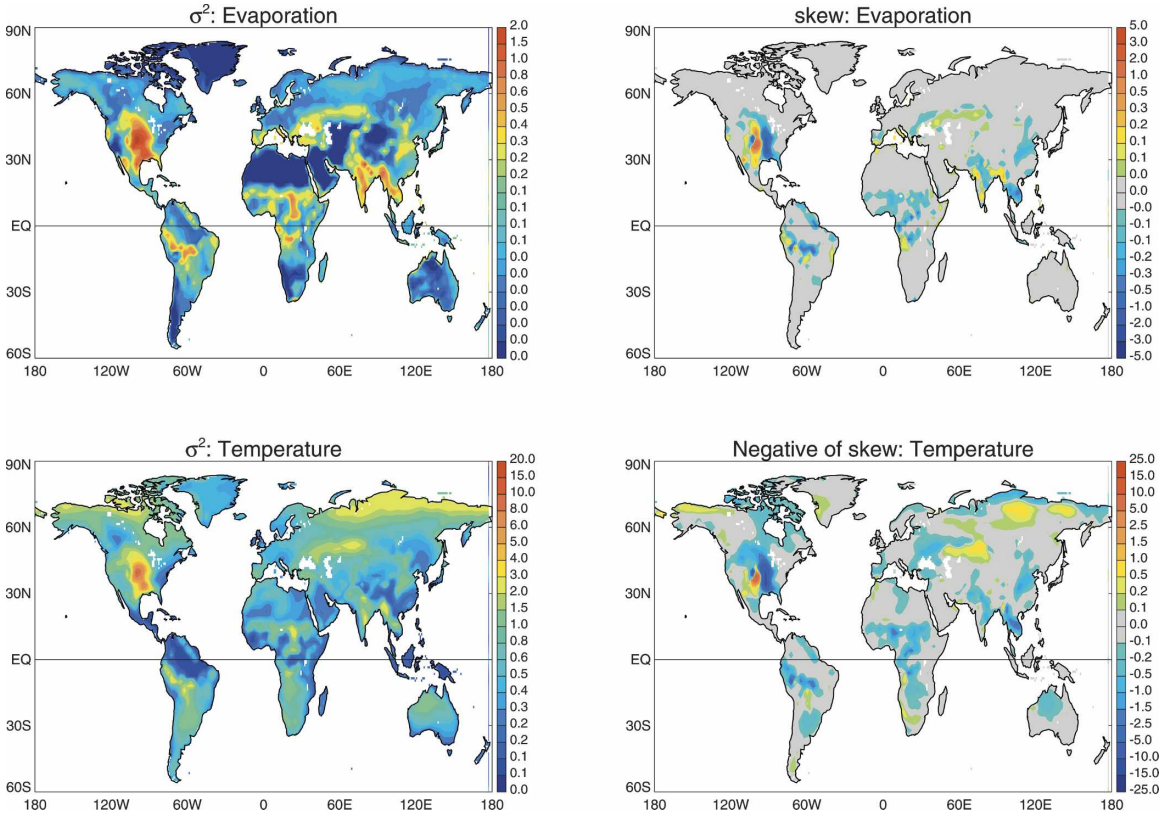

FIG. 5. (top left) Variance of seasonal (JJA) evaporation totals ($mm^2\ day^{-2}$). (top right) Skew of seasonal (JJA) evaporation totals ($mm^3\ day^{-3}$). (bottom) Corresponding plots for seasonally averaged air temperature in K^2 and K^3, respectively.

drological formulations. Their presence in the observational data can be considered a much more difficult test, one that indeed reflects on the correctness of the imposed formulations and on the importance of feedback in the real world.

a. Available data

Gridded temperature data were derived from point measurements archived by GHCN (Peterson and Vose 1997). More precisely, we used the homogeneity-adjusted form of the "version 2" GHCN temperature dataset, as outlined on the Web site of the National Climatic Data Center (http://www1.ncdc.noaa.gov/pub/data/ghcn/v2/readme.temperature.Z). Individual measurements tagged as having failed a quality check were not considered in the analysis.

The point data (consisting of monthly averaged temperatures) were processed as follows. First, all stations within a given 2° × 2.5° grid cell were identified. (A 2° × 2.5° grid is chosen both for consistency with the AGCM data and to allow a detailed representation of the moments' spatial structures.) For each station n within the grid cell, the mean JJA temperature over all years was computed and then subtracted from that station's individual JJA values to produce a time series of anomalies, $T'_{t,n}$. The grid cell average JJA temperature anomaly for each year t, $T_{t,\mathrm{grid}}$, was computed as the simple average of $T'_{t,n}$ over the N_t stations within the cell that contribute during that year. Note that simply averaging together all of the JJA temperatures in a given year over the stations in a grid cell and then computing a time series of anomalies from the resulting time series of temperatures would produce a different—and much less defensible—result, since the different stations have different record lengths and are affected differently by elevation, aspect, etc. By computing the anomalies for each station separately and then averaging the anomalies, we account for the fact that N_t varies with time.

Individual measurements, of course, are subject to error, so a grid cell average should be based on as many measurements as possible. In addition, many years of data are necessary to provide accurate estimates of the higher temperature moments. Balancing these two requirements helped us define criteria for constructing our gridded temperature dataset. If more than three stations within a grid cell were required to generate a grid cell value, coverage across the United States (the

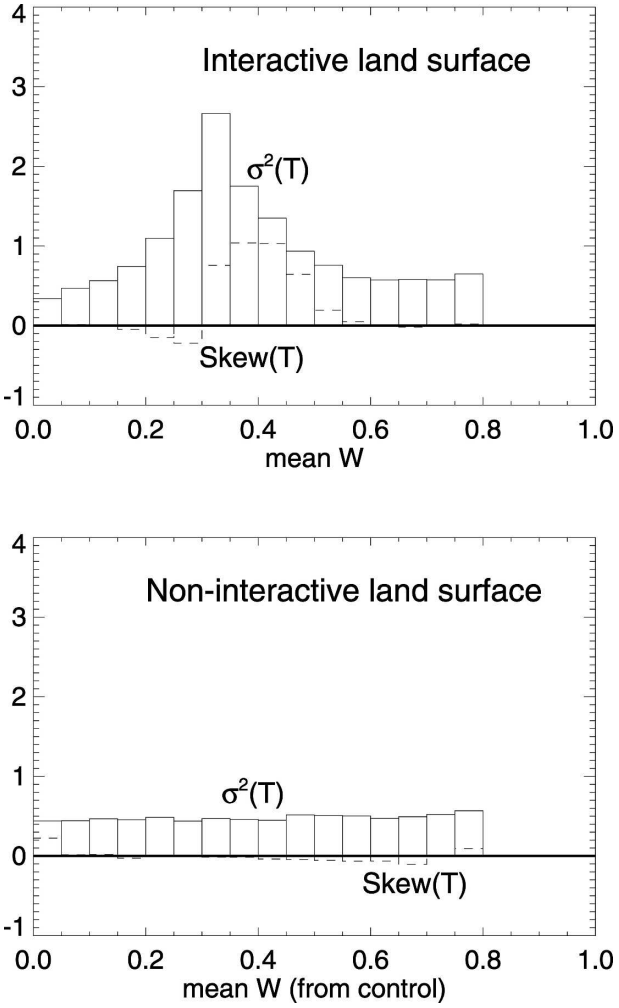

FIG. 6. (top) Variance (K^2) and skew (K^3) of seasonal (JJA) temperature as a function of mean soil moisture. (bottom) Same as top, but from an AGCM run in which land–atmosphere feedback is disabled.

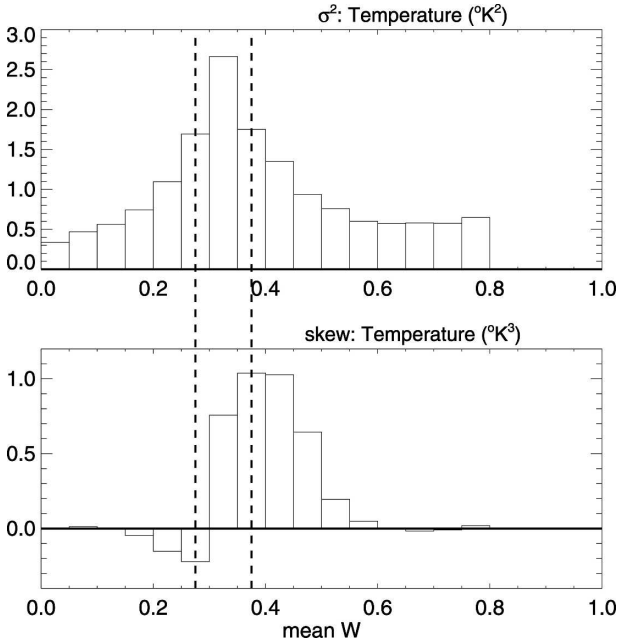

FIG. 7. (top) Variance of seasonal (JJA) temperature as a function of mean soil moisture. (bottom) Skew of seasonal (JJA) temperature as a function of mean soil moisture.

only large-scale region with comprehensive coverage) would be largely incomplete for any reasonable minimum number of sample years, making map comparison difficult. We thus require three station measurements to compute an average grid cell value. The coverage across the United States under this criterion is reasonable for a minimum sample size of 75 but falls off for minimum sample sizes much larger than this; thus, we impose a minimum of 75 yr of data to compute the temperature moments. Figure 8a shows the locations across the globe where gridded temperature moments can be computed under these two criteria. Again, for map comparisons, we focus in this paper on the North American region encompassing the continental United States. Thus, for the map comparisons, we effectively focus on temperature data from the U.S. Historical Climate Network (USHCN), since the USHCN data effectively constitute the U.S. subset of the GHCN temperature data. Fortunately, much more than 75 yr of data are typically available across the United States, as indicated in Fig. 8b.

Long-term soil moisture records are even more meager. Outside of spatial interpolations between point measurements in Asia and retrievals of soil moisture in the top centimeter of the earth from satellite, direct, decadal estimates of observational soil moisture data at regional to continental scales do not exist. Useful proxies, however, are available. Most notably, global offline land model simulations, when driven with observed meteorological forcings, provide a comprehensive set of soil moisture data at depth. Although the absolute magnitudes of model-generated soil moisture will typically differ from the observations, the model should compute realistically the soil moisture's temporal variability (Entin et al. 1999) and thus its higher statistical moments. Here, we use a 15-yr soil moisture dataset obtained by driving the Mosaic land surface model (the land model used in the AGCM analysis above) with 15-yr European Centre for Medium-Range Weather Forecasts (ECMWF) Re-Analysis (ERA-15) forcing that was corrected on the monthly scale (Berg et al. 2003) with GPCP precipitation data (Adler et al. 2003) and SRB radiation data (Gupta et al. 1999). The generation of these offline land surface data is described in more de-

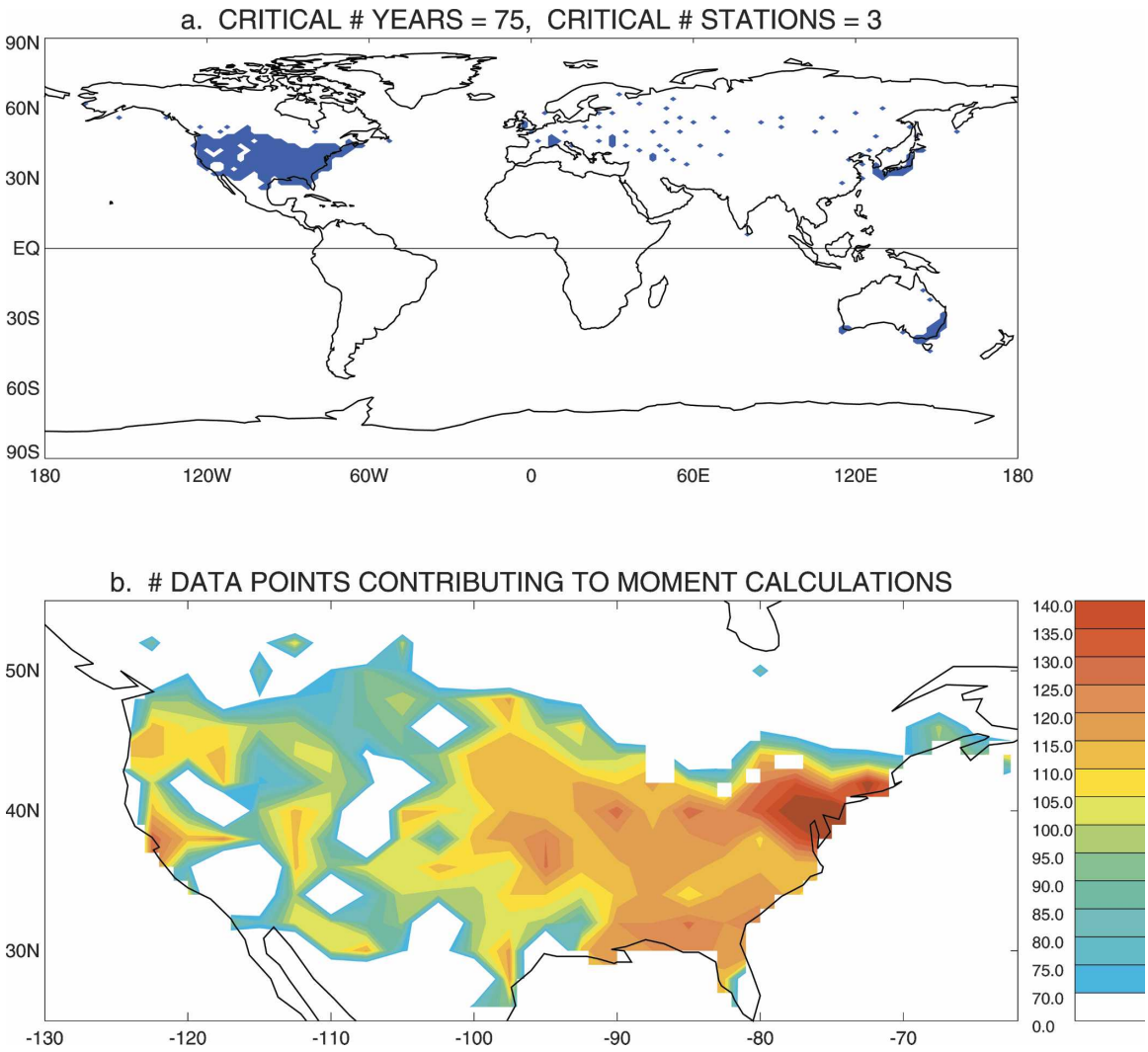

FIG. 8. (a) Map of the locations for which available observations allow an adequate estimation of gridded temperature moments. (b) Number of data points upon which the temperature moment calculations in the continental United States were based.

tail by Mahanama and Koster (2005). Although 15 yr of JJA averages are unquestionably insufficient for estimating soil moisture skew, they can provide a useful first-order estimate of soil moisture variance.

b. Observational results

The observational results are summarized in the histogram in Fig. 9, which is constructed using all of the available Northern Hemisphere midlatitude points indicated in Fig. 8a, not just those in the United States. In the plot, the maximum of temperature skew does lie on the wet side of the temperature variance maximum, which itself lies on the dry side of the soil moisture variance maximum. The skew never appears negative in this plot, but it does show a local minimum on the dry side of the temperature variance maximum. The features in Fig. 9 are in general agreement with the signatures of soil moisture impact on air temperature moments outlined in section 3d.

Given the limited availability of the observational data, it is instructive to view these results in map form. The top two panels of Fig. 10 show the mean soil moisture (degree of saturation) over the United States for JJA as determined from the AGCM and the ECMWF-based observational proxy. Both maps—and especially the "observational" map, which is not influenced by an unrealistic precipitation maximum in the center of the country—show a strong west-to-east gradient of soil moisture. Thus, again, in the United States, saying that a feature is on the "dry side" of another feature generally means that it lies to the west. Notice that the

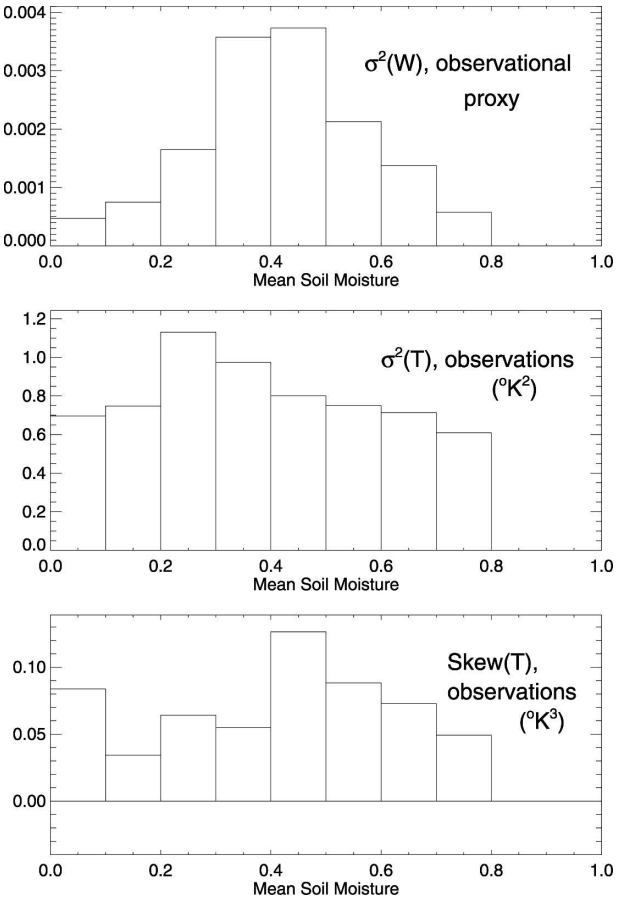

FIG. 9. (top) "Observed" soil moisture variance vs "observed" mean soil moisture. Observational soil moisture proxies are obtained by driving a land surface model with observations-based meteorological forcing. (middle) Temperature variance, as determined from GHCN temperature data, vs mean (proxy) soil moisture. (bottom) Temperature skew, as determined from GHCN temperature data, vs mean (proxy) soil moisture. Given the reduced data volume relative to that underlying Figs. 3 and 4, the bin width used here is 0.1.

maximum of the "observed" soil moisture variance [$\sigma^2(w_{\text{obs}})$; Fig. 10c] appears, as expected from Fig. 1, at intermediate mean soil moisture values. Part of the variance structure takes the form of a "bull's-eye," reflecting a similar bull's-eye in the observed summer precipitation variance field (e.g., Koster et al. 2003). Keep in mind that the limited time series give imperfect estimates of the true underlying variances, Monte Carlo sampling of a perfect normal distribution suggests that with 15 sampling points, the RMSE of the estimated soil moisture variance is roughly 37% of the true variance.

Figure 11c shows the distribution of the observed temperature variance $\sigma^2(T_{\text{obs}})$ in the United States. (Monte Carlo analysis shows that for the minimum 75 sampling points considered here, the RMSE of the temperature variance estimates, assuming an underlying normal distribution, is roughly 16% of the true variance.) The dots indicate grid cells for which the "observed" soil moisture variance (from Fig. 10c) exceeds 0.005. The positioning of the $\sigma^2(T_{\text{obs}})$ maximum on the dry side of the $\sigma^2(w_{\text{obs}})$ maximum—one of the hydrological signatures identified in section 3d—is very clear. Perhaps even more convincing (since the observational proxy soil moistures are not needed) is the comparison of Fig. 11c with the top two panels of the figure, which show the temperature variance distributions obtained from the control AGCM simulations and from the fixed-β simulation (discussed in conjunction with Fig. 6). The control simulations' variances are much too large relative to observations. Nevertheless, the pattern of the simulated variance distribution agrees quite well with that of the observed distribution. In the AGCM, this pattern disappears when land–atmosphere feedback is artificially prevented (Fig. 11b). Thus, either the agreement in the patterns in Figs. 11a and 11c is a coincidence, or feedback does determine the temperature variance distribution in the real world.

Feedback by itself, however, is not enough—the nonlinearity of the soil moisture/evaporation fraction relationship is also needed to produce this variance signature. Interestingly, the model calculations of Huang et al. (1996; see their Fig. 2) show an evaporation variance maximum (and thus, presumably, a temperature variance maximum) roughly coincident with a soil moisture variance maximum in the central United States, in contrast to the findings presented here. Note, however, that the model used by Huang et al. (1996) relates evaporation linearly to soil moisture—the plateau and associated nonlinearity seen in Fig. 2 of the present paper is not assumed. It is the nonlinearity induced by the plateau that causes the westward shift in the evaporation (and temperature) variance relative to the soil moisture variance in our model simulations (Fig. 3) and apparently in the real world (Fig. 11c).

Figure 12 shows, for the continental United States, the skew of JJA temperature for the control simulations, for the fixed-β simulation, and for the observations. Note that the estimation of skew from 50 data points (for the fixed-β simulation) or 75 data points (for the observations) carries with it much uncertainty. To facilitate the comparison in the presence of such sampling error—to weed out the substantial noise in the figures—any grid cell with a skew not significantly different from zero at the 80% confidence level (as determined from Monte Carlo analysis considering coefficient of skewness) is whited out. The great majority of

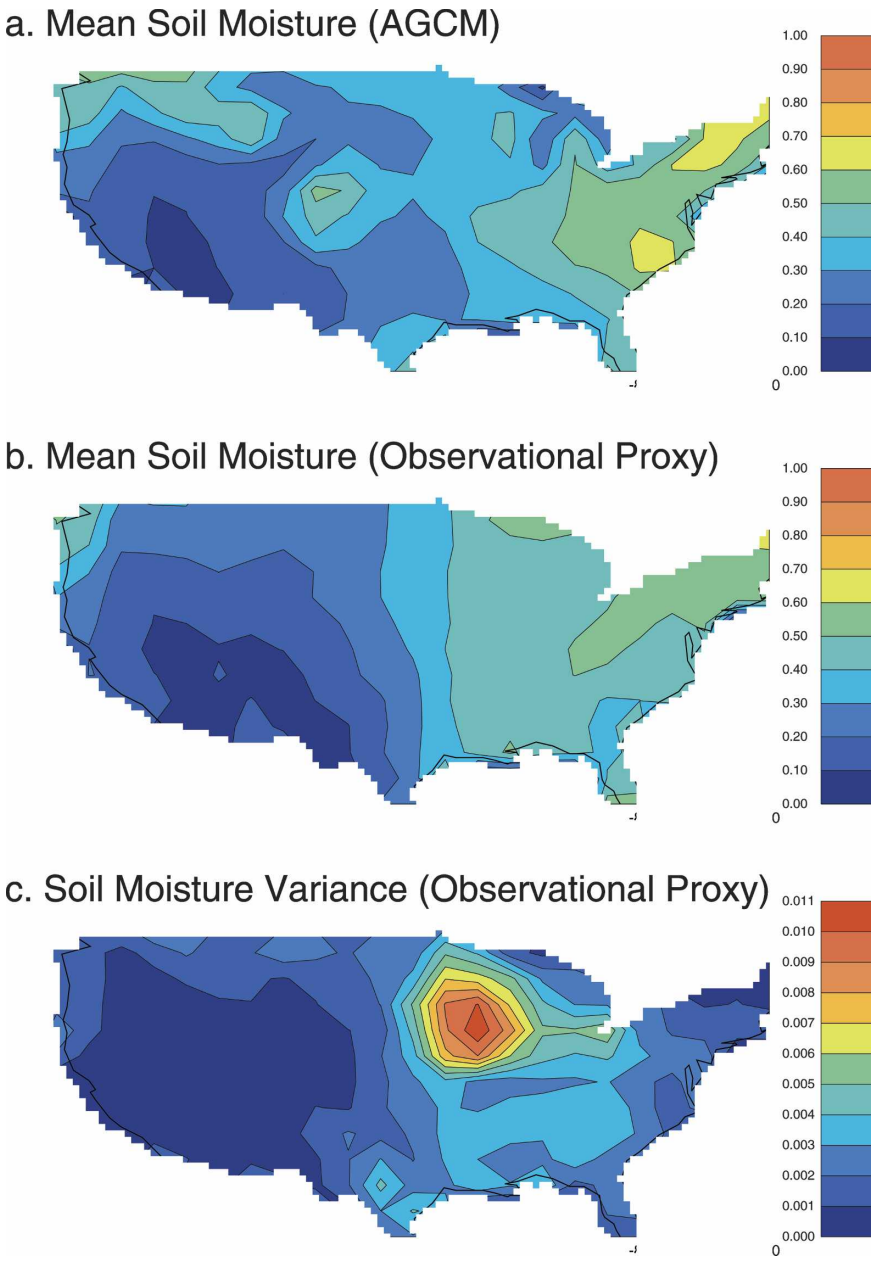

FIG. 10. (a) Mean soil moisture in the root zone (expressed as a degree of saturation) for JJA, as computed by the AGCM–land surface model (LSM) simulations. (b) Same as (a), but for the land surface model driven offline by realistic observational forcing spanning 15 yr. (c) Variance of root zone soil moisture, as determined in the 15-yr offline simulation.

the grid cells for the fixed-β and observational analyses show skews that are statistically indistinguishable from zero. Note that a skew can be close to zero and still have a coefficient of skewness that is statistically significant, which explains the presence of some gray patches in the figures.

The stronger of the two skew-related hydrological signatures on air temperature can be seen in the observational data. The dots in the bottom panel of Fig. 12 locate the observed temperature variance maximum from Fig. 11c [showing where $\sigma^2(T_{\text{obs}})$ exceeds 1.1 K^2]. In accordance with Fig. 7, a significant region of positive skew appears on the wet side of the variance maximum, toward the southeast. Its appearance there could, of course, be a reflection of sampling error; for example, the similarly sized region of negative skew pro-

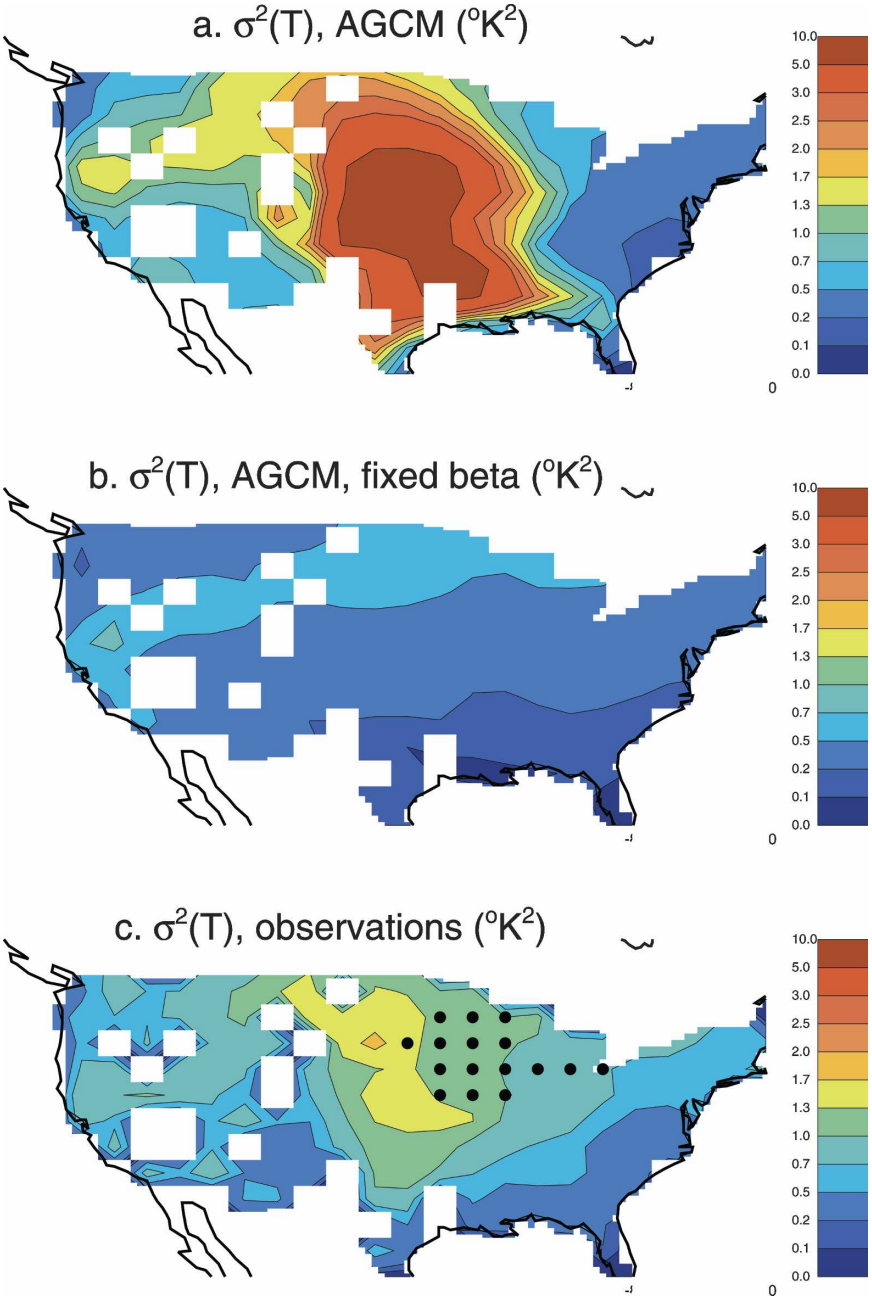

FIG. 11. (a) Variance of JJA air temperature, as obtained from the AGCM control simulations. (b) Same as (a), but for the AGCM fixed-β simulation, in which land–atmosphere feedback is artificially suppressed. (c) Same as (a), but for the GHCN observations. The dots show where the "observed" soil moisture variance (from the observational proxy) exceeds 0.005. Whited-out areas are regions of inadequate station coverage.

duced in the fixed-β simulation (middle panel) is presumably consistent with that plot's field significance levels. Nevertheless, the fact that the positive skew region appears where expected from basic hydrological considerations supports the idea that it is a real signal. Notice also that a hint of a negative skew appears where expected on the dry side of the variance maximum, though this signal is too small to merit much consideration. The substantial signal in the AGCM (Fig. 12a) disappears in the fixed-β run, again showing that the signal in the AGCM, and thus possibly in the observations, is indeed induced by feedback.

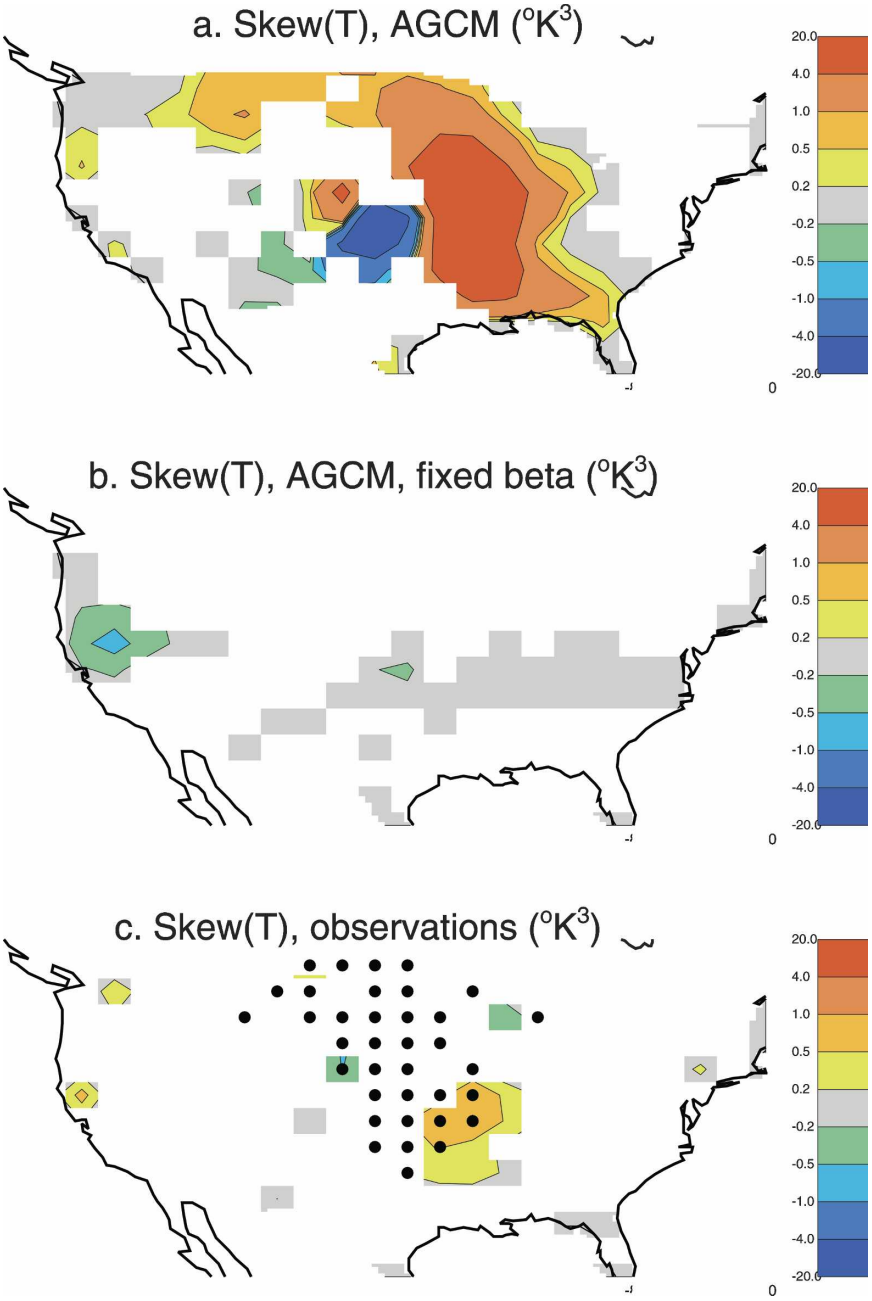

FIG. 12. (a) Skew of JJA air temperature, as obtained from the AGCM control simulations. (b) Same as (a), but for the AGCM fixed-β simulation, in which land–atmosphere feedback is artificially suppressed. (c) Same as (a), but for the GHCN observations. The dots show where the observed air temperature variance exceeds 1.1 K^2. Whited-out areas either have inadequate station coverage or have skews that are statistically indistinguishable from zero at the 80% confidence level.

5. Summary and discussion

GHCN observations show that seasonal (JJA) air temperatures have a maximum variance in the central Great Plains (Fig. 11c), on the dry side of a soil moisture variance maximum determined from an observational proxy. The map of observed temperature skew (bottom panel of Fig. 12) suggests that temperature extremes in a region centered around Arkansas and Missouri (on the wet side of the temperature variance

maximum) will tend to be warm rather than cool. The same general behavior (in pattern, though not in magnitude) is also seen in the AGCM; the simulated extrema in the moments are located geographically in roughly the same places (Figs. 11a and 12a). The underlying relationships between mean soil moisture and the temperature moments appear to be about the same in the observations and the model (Figs. 3, 4, and 9).

The AGCM's behavior is intuitively explained by simple hydrological mechanisms, mechanisms that are fully supported by the joint analysis of AGCM soil moisture, evaporation, and temperature fields. Figures 6, 11, and 12 provide further evidence for these mechanisms—when land–atmosphere interaction is artificially disabled, the relationships between the temperature moments and mean soil moisture disappear. The agreement between the observational and control model results suggests that the identified mechanisms are also operating in nature.

Shorter, such as daily, time scales are not addressed here; presumably the relationships involved at shorter time scales would be much more complex, since temperatures at these time scales would be influenced more by synoptic weather patterns. Also, the moments examined are not strongly affected by long-term (decadal) trends, despite evidence for such trends in measured time series of such variables as precipitation and potential evaporation (e.g., Lawrimore and Peterson 2000). When the observational temperature data at each grid cell is regressed against time and the resulting linear trend is subtracted from the grid cell's temperature time series, the resulting moments (not shown) are very close to those shown in Figs. 11 and 12. Again, this paper focuses on soil moisture/air temperature feedback at seasonal time scales.

The comparisons in Figs. 3, 4, 9, 11, and 12, in conjunction with the hydrological analysis outlined in section 3, give us reason to believe that the seasonal (JJA) variance and skew distributions seen in the observational air temperature record are largely explained by basic subsurface hydrological processes, namely, by the nonlinear relationship between evaporation and soil moisture and by the moments in soil moisture induced by its unavoidable upper and lower bounds. In other words, through the use of a long-term observational dataset—the GHCN air temperature dataset—this study provides further support for the supposition that land moisture variables have a first-order impact on the temporal variability of meteorological fields on seasonal time scales.

Acknowledgments. We thank three anonymous reviewers for helpful comments. The AGCM runs were funded by the Earth Science Enterprise of NASA Headquarters through the EOS-Interdisciplinary Science Program and the NASA Global Modeling and Assimilation Office (GMAO), with computational resources provided by the NASA Center for Computational Sciences. Ping Liu and Sarith Mahanama assisted with the data processing.

REFERENCES

Adler, R. F., and Coauthors, 2003: The version-2 Global Precipitation Climatology Project (GPCP) monthly precipitation analysis (1979–present). *J. Hydrometeor.,* **4,** 1147–1167.

Bacmeister, J., P. J. Pegion, S. D. Schubert, and M. J. Suarez, 2000: Atlas of seasonal means simulated by the NSIPP 1 atmospheric GCM. NASA Tech. Memo. 2000-104606, Vol. 17, 194 pp.

Beljaars, A. C. M., P. Viterbo, M. Miller, and A. K. Betts, 1996: The anomalous rainfall over the United States during July 1993: Sensitivity to land surface parameterization and soil moisture anomalies. *Mon. Wea. Rev.,* **124,** 362–383.

Berg, A. A., J. S. Famiglietti, J. P. Walker, and P. R. Houser, 2003: Impact of bias correction to reanalysis products on simulations of North American soil moisture and hydrological fluxes. *J. Geophys. Res.,* **108,** 4490, doi:10.1029/2002JD003334.

Budyko, M. I., 1974: *Climate and Life.* Academic Press, 508 pp.

Chou, M.-D., and M. Suarez, 1994: An efficient thermal infrared radiation parameterization for use in general circulation models. NASA Tech. Memo. 104606, Vol. 3, 84 pp.

——, and ——, 1996: A solar radiation parameterization (CLIRAD-SW) for atmospheric studies. NASA Tech. Memo. 104606, Vol. 15, 38 pp.

Delworth, T., and S. Manabe, 1989: The influence of soil wetness on near-surface atmospheric variability. *J. Climate,* **2,** 1447–1462.

Dirmeyer, P. A., 2000: Using a global soil wetness dataset to improve seasonal climate simulation. *J. Climate,* **13,** 2900–2922.

Douville, H., and F. Chauvin, 2000: Relevance of soil moisture for seasonal climate predictions: A preliminary study. *Climate Dyn.,* **16,** 719–736.

Eagleson, P. S., 1978: Climate, soil and vegetation. 4. The expected value of annual evapotranspiration. *Water Resour. Res.,* **14,** 731–739.

Entin, J. K., A. Robock, K. Y. Vinnikov, V. Zabelin, S. Liu, A. Namkhai, and T. Adyasuren, 1999: Evaluation of Global Soil Wetness Project soil moisture simulations. *J. Meteor. Soc. Japan,* **77,** 183–198.

Fennessy, M. J., and J. Shukla, 1999: Impact of initial soil wetness on seasonal atmospheric prediction. *J. Climate,* **12,** 3167–3180.

Guo, Z., Coauthors, 2006: GLACE: The Global Land–Atmosphere Coupling Experiment. Part II: Analysis. *J. Hydrometeor.,* **7,** 611–625.

Gupta, S. K., N. A. Ritchey, A. C. Wilber, C. H. Whitlock, G. G. Gibson, and P. W. Stackhouse Jr., 1999: A climatology of surface radiation budget derived from satellite data. *J. Climate,* **12,** 2691–2710.

Higgins, R. W., W. Shi, and E. Yarosh, 2000*: Improved United States Precipitation Quality Control System and Analysis.* NCEP/Climate Prediction Center Atlas 7, 40 pp. [Available online at http://www.cpc.ncep.noaa.gov/research_papers/-ncep_cpc_atlas/7/index.html.]

Huang, J., and M. H. Van den Dool, 1993: Monthly precipitation–temperature relations and temperature prediction over the United States. *J. Climate,* **6,** 1111–1132.

——, ——, and K. P. Georgakakos, 1996: Analysis of model-calculated soil moisture over the United States (1931–1993) and applications to long-range temperature forecasts. *J. Climate,* **9,** 1350–1362.

Koster, R. D., and M. Suarez, 1996: Energy and water balance calculations in the Mosaic LSM. NASA Tech. Memo. 104606, Vol. 9, 59 pp.

——, and P. C. D. Milly, 1997: The interplay between transpiration and runoff formulations in land surface schemes used with atmospheric models. *J. Climate,* **10,** 1578–1591.

——, and M. J. Suarez, 2004: Suggestions in the observational record of land–atmosphere feedback operating at seasonal timescales. *J. Hydrometeor.,* **5,** 567–572.

——, ——, and M. Heiser, 2000: Variance and predictability of precipitation at seasonal-to-interannual timescales. *J. Hydrometeor.,* **1,** 26–46.

——, ——, R. W. Higgins, and H. Van den Dool, 2003: Observational evidence that soil moisture variations affect precipitation. *Geophys. Res. Lett.,* **30,** 1241, doi:10.1029/2002GL016571.

——, and Coauthors, 2004: Realistic initialization of land surface states: Impacts on subseasonal forecast skill. *J. Hydrometeor.,* **5,** 1049–1063.

——, and Coauthors, 2006: GLACE: The Global Land–Atmosphere Coupling Experiment. Part I: Overview. *J. Hydrometeor.,* **7,** 590–610.

Lawrimore, J. H., and T. C. Peterson, 2000: Pan evaporation trends in dry and humid regions of the United States. *J. Hydrometeor.,* **1,** 543–546.

Mahanama, S. P. P., and R. D. Koster, 2005: AGCM biases in evaporation regime: Impacts on soil moisture memory and land–atmosphere feedback. *J. Hydrometeor.,* **6,** 656–669.

Manabe, S., 1969: Climate and the ocean circulation. I. The atmospheric circulation and the hydrology of the earth's surface. *Mon. Wea. Rev.,* **97,** 739–774.

Moorthi, S., and M. J. Suarez, 1992: Relaxed Arakawa–Schubert: A parameterization of moist convection for general circulation models. *Mon. Wea. Rev.,* **120,** 978–1002.

Peterson, T. C., and R. S. Vose, 1997: An overview of the Global Historical Climatology Network temperature data base. *Bull. Amer. Meteor. Soc.,* **78,** 2837–2849.